



# PREPARATION, CHARACTERIZATION AND BIOLOGICAL ACTIVITY OF NOVEL SCHIFF BASE COMPLEXES BASED ON La, Er and Yb METAL IONS

Hoda A. Elsayy<sup>1</sup>, Walaa H. Mahmoud<sup>2</sup>, Islam M. Al-Akraa<sup>1</sup> and Gehad G. Mohamed<sup>2,3</sup>

<sup>1</sup>Chemical Engineering Department, Faculty of Engineering, The British University in Egypt, Cairo, Egypt

<sup>2</sup>Chemistry Department, Faculty of Science, Cairo University, Giza, Egypt

<sup>3</sup>Egypt Nanotechnology Center, 6<sup>th</sup> October City, El-Sheikh Zayed, Giza, Egypt

E-Mail: [Hoda.ahmed@bue.edu.eg](mailto:Hoda.ahmed@bue.edu.eg)

## ABSTRACT

The tridentate [HL, (4-[(2-(2-quinolinoimino)-3, 5-dibromobenzyl) amino] cyclohexanol]Schiff base ligand was prepared from the condensation reaction of 2-quinoline carbaldehyde with the drug ambroxol. The prepared HL ligand was further used in the preparation of some new complexes via the reaction with La(III), Er(III) and Yb(III) metal ions. The geometry of the prepared complexes was proposed from elemental analysis, FT-IR, <sup>1</sup>H NMR, thermal and magnetic susceptibility. <sup>1</sup>H NMR showed that the three nitrogen atoms of the ligand were responsible for the complex formation. The thermal analysis technique provided a clear prospect about the decomposition steps of the Schiff base ligand and its complexes; as it also showed the number of water molecules present in the inner and outer coordination sphere of the prepared complexes. Upon these studies, an octahedral geometry for all of the complexes has been proposed. The Schiff base and its complexes have been screened for their antimicrobial activity. The biological activity results deduced that Er(III) complex possesses the highest activity.

**Keywords:** ambroxol, FT-IR, <sup>1</sup>H NMR, antimicrobial activity.

## 1. INTRODUCTION

Recently a major interest has developed for the synthesis of Schiff base ligands as well as their transition metal complexes. Evidently, Novel transition metal complexes of this type require the preparation of a new Schiff base ligand as an initial step, where the newly synthesized ligand would acquire unique properties and distinctive reactivity (Abdel-Monem *et al.*, 2018). Schiff base ligands possess very interesting qualities and have been extensively employed in coordination chemistry, they are simply the condensation reaction product of a primary amine with a carbonyl group (of either aldehyde or a ketone), to form the azomethine functional group(Slassi *et al.*, 2019). Basically, due to the simplicity of their preparation, their flexibility as well as the vast range of their coordination ability, Schiff base ligands have gained a huge popularity in the field of metal complexes and coordination chemistry(Alshaheri *et al.*, 2017). Moreover, recent studies have confirmed that the efficiency of metal complexes based on biologically significant ligands are often more prominent than that of the free ligand form(Arulmurugan *et al.*, 2010). Usually, Schiff base ligands are basically employed to act as bi- or tridentate ligands, however, it was very recently found that the tridentate Schiff base ligands with a flexible atom, compared to their bidentate counterparts, are more efficient in coordination of transition metals, as confirmed by the values of their stability constants, which is mainly attributed to the additional coordination of an extra donating atom (Diab *et al.*, 2017).

A vast range of biological applications have been reported in literature about Schiff base ligands as well as their respective metal complexes. Various applications incorporate antibacterial, antifungal, anticancer, anti-

inflammatory as well as antiviral activity. It is also very worth mentioning that they possess a very prominent catalytic activity in several chemical reactions (Arulmurugan *et al.*, 2010; Zoubi and Ko, 2017).

The chemistry of lanthanide coordination has been a very significant point of research. Their unique and distinctive molecular structures can play an important role in a variety of techniques such as investigative applications in biology, catalysis, luminescence and magnetism which asserted the importance and the prospective value of this area of research (Gueye *et al.*, 2017).

Ambroxol, a drug which has been used before as a mucolytic agent, i.e. a muco-active substance used in treating acute and chronic bronchitis; has been also found to exhibit a range of other interesting applications as an antioxidant and an anti-inflammatory. It has also been reported to help in impairing the conduction of sodium ion. It is also known to induce the process of secretion of surfactants as well as causing expectorant effects by diminishing the linkage between the mucus and the bronchial of the lining (Mahmoud *et al.*, 2017; Rajesh *et al.*, 2017).

In this present work, a new Schiff base based on the drug ambroxol as a primary amine was prepared by condensation with 2-quinoline carbaldehyde. Purification and full characterization of the ligand was conducted, followed by the synthesis of metal complexes based on the newly prepared ligand and Lanthanides. Experimental approaches to study the structure of the newly formed ambroxol Schiff base ligand as well as its synthesized Lanthanide metal complexes have been investigated. Also, their antimicrobial activity against several types of bacteria and fungi has been screened and investigated.



## 2. EXPERIMENTAL

### 2.1 Materials, reagents, and solutions

Analytical grade chemicals of high purity were used in this study. Ambroxol was provided from Nile Pharma while 2-hydroxybenzaldehyde, LaCl<sub>3</sub>.7H<sub>2</sub>O, YbCl<sub>3</sub>.7H<sub>2</sub>O and ErCl<sub>3</sub>.7H<sub>2</sub>O were provided from Sigma Aldrich. Ethyl alcohol (99 and 95%) has been used as an organic solvent and in all preparations where is applicable, deionized water was used. Fresh stock solution of (1x10<sup>-3</sup> M) HL ligand was prepared by dissolving 0.4 g in a suitable volume of ethyl alcohol. Then 1x10<sup>-4</sup> M and 1x10<sup>-5</sup> M solutions of the Schiff base ligand and its metal complexes were prepared by appropriate dilution from the previously prepared stock solutions.

### 2.2 Instruments

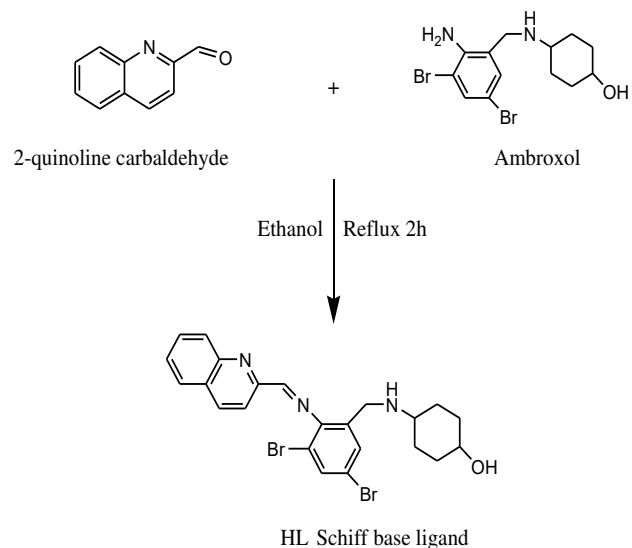
Microanalyses of carbon, hydrogen and nitrogen were carried out using CHNS-932 (LECO) Vario Elemental Analyzer. Analyses of the metals followed the dissolution of the solid complexes in concentrated HNO<sub>3</sub>, neutralizing the diluted aqueous solutions with ammonia and titrating the metal solutions with EDTA. FT-IR spectra were recorded on a Perkin-Elmer 1650 spectrometer (4000-400 cm<sup>-1</sup>) in KBr pellets. The thermogravimetric analyses (TG and DTG) of the solid complexes were carried out from room temperature to 1000°C using a Shimadzu TG-50H thermal analyzer.

### 2.3 Synthesis of Schiff base ligand (HL)

The Schiff base ligand (HL) was prepared by refluxing the ambroxol drug (6.61 mmol, 2.5 g), dissolved in ethanol, with 2-quinoline carbaldehyde (6.61 mmol, 1.04 g). The resulting Schiff base was stirred under reflux for about 2h. During that, a reddish brown solid compound was obtained and separated (Scheme 1) then it was filtered, recrystallized and washed with DMF and dried in vacuum.

### 2.4 Synthesis of the metal complexes

The metal complexes were synthesized by the addition of the appropriate metal chloride (0.77 mmol) in ethanol (25 mL) to the hot solution (60 °C) of the HL ligand (0.4 g/L, 0.77 mmol) in ethanol (25 mL). The obtained mixture was stirred under reflux for two hours during which the complexes precipitated. The complexes then removed by filtration, washed with a little amount of hot DMF and dried in vacuum desiccator over anhydrous calcium chloride. The analytical data for C, H and N were repeated twice.



**Scheme-1.** Preparation of the HL Schiff base ligand.

### 2.5 Biological activity

A filter paper disk (5 mm) was transferred into 250 ml flasks containing 20 mL of working volume of tested solution (100 mg/mL). All flasks were autoclaved for 20 min at 121°C. LB agar media surfaces were inoculated with four investigated bacteria (Gram positive bacteria: *Bacillus Subtilis* and *Streptococcus pneumoniae*; Gram negative bacteria: *Salmonella* species and *Escherichia coli*) and fungi (*Aspergillus fumigatus* and *Candida albicans*) by diffusion agar technique then, transferred to a saturated disk with a tested solution in the center of Petri dish (agar plates). All the compounds were placed at 4 equidistant places at a distance of 2 cm from the center in the inoculated Petri plates. DMSO served as control. Finally, all these Petri dishes were incubated at 25°C for 48 h where clear or inhibition zones were detected around each disk. Control flask of the experiment was designed to perform under the same condition described previously for each microorganism but with dimethylformamide solution only and by subtracting the diameter of inhibition zone resulting with dimethylformamide from that obtained in each case, so antibacterial activity could be calculated (Deghadi *et al.*, 2016). Amikacin and ketokonazole were used as reference compounds for antibacterial and antifungal activities, respectively. All experiments were performed as triplicate and data plotted were the mean value.

## 3. RESULTS AND DISCUSSIONS

### 3.1 Characterization of metal complexes

The complexes were characterized by different techniques such as elemental analyses, IR spectral, molar conductance, and thermal analyses.

#### 3.1.1 Elemental analysis

Metal complexes of Schiff base were prepared by the reaction of the ethanoic solutions of Schiff base and metal salt in 1:1 ratio and they had the composition of



MHL type. The experimental elemental analysis of complexes was very compatible with the theoretical calculations. The data of the elemental analyses of metal

complexes (C, H, N, Cl and M) with its molecular formula and the melting points were demonstrated in Table-1.

**Table-1.** Analytical and physical data of HL ligand and its metal complexes.

Compound (Molecular Formula)	Color (% yield)	M.P. (°C)	% Found (Calcd)					$\mu_{\text{eff.}}$ (B.M.)
			C	H	N	Cl	M	
[HL]	Reddish brown (92)	140	55.21 (55.38)	4.24 (4.45)	8.02 (8.13)	-----	-----	
[La(HL)(H <sub>2</sub> O) <sub>2</sub> Cl]Cl <sub>2</sub> .2H <sub>2</sub> O	Black (77)	175	33.00 (33.07)	3.62 (3.71)	4.86 (5.03)	12.47 (12.76)	16.54 (16.66)	Diam.
[Er(HL)(H <sub>2</sub> O)Cl <sub>2</sub> ].Cl	Brown (89)	165	34.02 (34.12)	2.94 (3.09)	5.03 (5.19)	13.07 (13.17)	20.45 (20.65)	Diam.
[Yb(HL)(H <sub>2</sub> O)Cl <sub>2</sub> ]Cl.3H <sub>2</sub> O	Brown (85)	161	31.65 (31.78)	3.34 (3.57)	4.62 (4.84)	12.09 (12.26)	19.74 (19.92)	Diam.

### 3.1.2 Molar conductance measurements

In the complexation process, HL Schiff base acted as a neutral tridentates ligand. The molar conductance was measured by dissolving 10<sup>-3</sup> M of the ligand in ethanol at 25 °C by using the recommended procedure (Cakir *et al.*, 2003). Yb(III) and Er(III) complexes showed molar conductance values of 61 and 74 Ω<sup>-1</sup> mol<sup>-1</sup> cm<sup>2</sup>, respectively, indicated the ionic nature of these complexes and they were of the type 1:1 electrolytes. While in case of La(III) complex, it was found to be 104 Ω<sup>-1</sup> mol<sup>-1</sup> cm<sup>2</sup> which indicated its electrolytic nature.

### 3.1.3 Infrared spectra and mode of bonding

The IR spectra of the formed complexes were compared with those of the free ligand to distinguish the coordination sites of chelation and the results obtained were listed in Table-2. The IR spectrum of HL ligand exhibited a band at 1630 cm<sup>-1</sup> resulting from the azomethine v(C=N) group (Ahmadi and Amani, 2012; Issa *et al.*, 2008). This band was shifted to lower wavelength in the spectra of all the complexes at the range of 1626-1629 cm<sup>-1</sup> indicating the involvement of azomethine nitrogen in the chelation to the metal ions (Jenisha *et al.*, 2015). It was hard to characterize the stretching band of v(NH) due to its overlapping with the v(OH) stretching vibration band. The stretching band of the pyridine ring was observed in the free ligand at 1074 cm<sup>-1</sup> which was shifted in all the formed complexes to appear at 1064-1066 cm<sup>-1</sup> indicating the participation of the pyridine ring in the complexation

process (El-Binary *et al.*, 2016). The v(NH) bending band was observed in the free ligand at 618 cm<sup>-1</sup> which was shifted in the La(III) complex to be observed at 612 cm<sup>-1</sup> while in both Er(III) and Yb(III) complexes it was observed at the same place of the ligand (618 cm<sup>-1</sup>), this may indicate the linkage between the metal ions and the nitrogen atom. A new bands in all complexes have appeared in the region 425-440 cm<sup>-1</sup> attributed to v(M-N) (More *et al.*, 2017). The bands presented in the region 510-553 cm<sup>-1</sup> in all the complexes were assigned to v(M-O) stretching vibration of coordinated water (Nassar *et al.*, 2018). As well as, two new bands of coordinated water molecules v(H<sub>2</sub>O) appeared in the IR spectra of metal complexes at 818-871 and 746-764 cm<sup>-1</sup>, indicating the binding of water molecules to the metal ions [25]. Accordingly, the HL ligand acted as a neutral tridentate chelating agent, bonded to the metal ion via three nitrogen atoms of the Schiff base. The formation of octahedral complexes was obtained through coordination with water molecules and chloride ions in all complexes.

### 3.1.4 Thermal analysis studies (TG and DTG)

Thermogravimetric technique (TG) and differential thermogravimetric (DTG) analyses were carried out for the Schiff base ligand (HL) as well as its metal complexes, with a scan over a temperature range from 50 to 1000 °C. All the results are presented in Table-3.

**Table-2.** IR spectra ( $4000\text{-}400\text{ cm}^{-1}$ ) data of HL ligand and its metal complexes.

HL	$[\text{La(HL)(H}_2\text{O)}_2\text{Cl}]Cl_2\cdot 2\text{H}_2\text{O}$	$[\text{Er(HL)(H}_2\text{O)Cl}_2]\text{Cl}$	$[\text{Yb(HL)(H}_2\text{O)Cl}_2]\text{Cl}\cdot 3\text{H}_2\text{O}$	Assignment
3422br	3390br	3359br	3405br	NH and OH
1630sh	1627sh	1626sh	1629m	C=N
1074m	1064m	1064m	1066sh	Pyridine ring stretching
-----	818w, 764w	835w, 746w	871w, 761s	$\text{H}_2\text{O}$ stretching of coordinated water
618s	612w	618w	618s	NH bending
-----	553w	510w	535w	M-O of coordinated water
-----	440w	430w	425w	M-N

sh = sharp, m = medium, br = broad, s = small, w = weak.

**Table-3.** Thermo analytical results (TG and DTG) of HL ligand and its metal complexes.

Complex	TG range ( $^{\circ}\text{C}$ )	DTGmax ( $^{\circ}\text{C}$ )	n*	Mass loss loss Estim (Calcd) %	Total mass loss % %	Assignment	Metallic residue
HL	50-300 300-605 605-1000	90, 225 450 730	2 1 1	26.01 (26.30) 43.24 (43.71) 30.26 (30.04) 99.51 (100.05)	26.01 (26.30) 43.24 (43.71) 30.26 (30.04) 99.51 (100.05)	Loss of $\text{C}_8\text{H}_{10}\text{NO}$ . Loss of $\text{C}_5\text{H}_6\text{Br}_2$ . Loss of $\text{C}_{10}\text{H}_7\text{N}_2$ .	----- - -
$[\text{La(HL)(H}_2\text{O)}_2\text{Cl}]Cl_2\cdot 2\text{H}_2\text{O}$	50-335 335-590 590-1000	75, 240 395 830, 870	2 1 2	37.45 (37.93) 14.17 (13.86) 29.27 (28.95)	37.45 (37.93) 14.17 (13.86) 29.27 (28.95) 80.89 (80.74)	Loss of $3\text{H}_2\text{O}$ and $\text{C}_4\text{H}_{13}\text{Cl}_3\text{BrN}$ . Loss of $\text{C}_8\text{H}_5\text{N}$ . Loss of $\text{C}_{16}\text{H}_{10}\text{Br}_2\text{NO}_{0.5}$ .	$\frac{1}{2}\text{La}_2\text{O}_3$
$[\text{Er(HL)(H}_2\text{O)Cl}_2]\text{Cl}$	50-310 310-600 600-1000	215 380 840, 880	1 1 2	20.01 (20.32) 26.89 (26.34) 29.27 (29.75) 76.17 (76.41)	20.01 (20.32) 26.89 (26.34) 29.27 (29.75) 76.17 (76.41)	Loss of $\text{C}_5\text{H}_8\text{Cl}_3\text{N}$ . Loss of $\text{C}_4\text{H}_5\text{Br}_2$ . Loss of $\text{C}_{16}\text{H}_{12}\text{N}_2\text{O}_{0.5}$ .	$\frac{1}{2}\text{Er}_2\text{O}_3$
$[\text{Yb(HL)(H}_2\text{O)Cl}_2]\text{Cl}\cdot 3\text{H}_2\text{O}$	50-150 150-430 430-1000	105 275 490, 680	1 1 2	6.61 (6.27) 46.37 (46.08) 25.02 (25.15)	6.61 (6.27) 46.37 (46.08) 25.02 (25.15) 78.00 (77.50)	Loss of $3\text{H}_2\text{O}$ . Loss of $\text{C}_{10}\text{H}_{13}\text{Cl}_3\text{Br}_2$ . Loss of $\text{C}_{13}\text{H}_{12}\text{N}_3\text{O}_{0.5}$ .	$\frac{1}{2}\text{Yb}_2\text{O}_3$

n\* = number of decomposition steps.

The TG data for the HL ligand showed a pattern of decomposition over four stages. The first two stages occurred within a temperature range of 50-300 °C, with temperature maxima at 90 and 225 °C. These values came into accordance with the evaluation of  $\text{C}_8\text{H}_{10}\text{NO}$  molecule corresponding to a mass loss of 26.01% (calculated mass loss = 26.30%). The third decomposition step occurred at a temperature maximum of 450 °C, which corresponds to the loss of  $\text{C}_5\text{H}_6\text{Br}_2$  molecule, with a mass loss of 43.24% (calculated mass loss = 43.71%). The final decomposition stage came within a temperature range of 605-1000 °C which correlates with a complete decomposition of the remaining part of the ligand ( $\text{C}_{10}\text{H}_7\text{N}_2$ ), the mass loss was found to be 30.26% (calculated mass loss = 30.04%). The DTG curve gave a maximum peak at 730 °C and the total weight loss amounted to 99.51% (calculated. 100.05%). The thermogram of  $[\text{La(HL)(H}_2\text{O)Cl}]Cl_2\cdot 2\text{H}_2\text{O}$  complex exhibited five stages of weight loss. The first two steps of decomposition have occurred within a temperature range of 50-335 °C with two maxima at 75 and 240 °C, that was

into accordance with the loss of three water molecules along with  $\text{C}_4\text{H}_{13}\text{Cl}_3\text{BrN}$  fragment with estimated mass loss of 37.45% (calculated mass loss = 37.93%). The third step of decomposition was detected in the range of 335-590 °C, and occurred at a temperature maximum of 395 °C corresponding to the loss of a  $\text{C}_8\text{H}_5\text{N}$  fragment, with estimated mass loss of 14.17% (calculated mass loss = 13.86%). The final two decomposition steps occurred in the temperature range of 590-1000 °C with two maxima at 830 and 870 °C, which in turn correspond to the loss of a  $\text{C}_{16}\text{H}_{10}\text{Br}_2\text{NO}_{0.5}$  fragment with estimated mass loss of 29.27% (calculated mass loss = 28.95%). Finally, a residue of  $\frac{1}{2}\text{La}_2\text{O}_3$  metal oxide remained. The overall weight loss amounted to 80.89% (calculated mass loss = 80.74%).

The thermal decomposition data of the  $[\text{Er(HL)(H}_2\text{O)Cl}_2]\text{Cl}$  complex exhibited four steps over a range of temperature from 50-1000 °C. The first decomposition step corresponds to an estimated mass loss of 20.01% (calcd. = 20.32%), which occurred within the temperature



range from 50-310 °C with a temperature maximum at 215 °C. This step might be attributed to the loss of C<sub>3</sub>H<sub>8</sub>Cl<sub>3</sub>N fragment. The next decomposition step occurred over a temperature range of 310-600 °C with a temperature maximum at 380 °C, in which the complex lost the organic fragment C<sub>4</sub>H<sub>5</sub>Br<sub>2</sub> with estimated mass loss of 26.89% (calcd. = 26.34%). The last two decomposition stages occurred over the temperature range of 600-1000 °C with two maxima at 840 and 880 °C, they were attributed to the loss of a C<sub>16</sub>H<sub>12</sub>N<sub>2</sub>O<sub>0.5</sub> fragment with estimated mass loss of 29.27% (calculated mass loss = 29.75%). Eventually, after the loss of the organic moiety, the metal oxide ½ Er<sub>2</sub>O<sub>3</sub> is expected to remain as the final product, with a total estimated mass loss of 76.17% (calcd. = 76.41%).

The thermogravimetric (TG) curve for [Yb(HL)(H<sub>2</sub>O)Cl<sub>2</sub>]Cl·3H<sub>2</sub>O complex exhibited pattern of weight loss over four stages of decomposition. The first step was observed within the temperature range of 50-150 °C, with a temperature maximum at 105 °C, that can be attributed to the loss of three water molecules of hydration, with estimated mass loss of 6.61% (calculated mass loss = 6.27%). On the other hand, the second stage of weight loss was observed within the temperature range of 150-430 °C, with a temperature maximum of 275 °C which may be related to the loss of an organic fragment C<sub>10</sub>H<sub>13</sub>Cl<sub>3</sub>Br<sub>2</sub>, that would amount to an overall estimated mass loss of 46.37% (calculated mass loss = 46.08%). The last two steps of decomposition occurred in the range of 430-1000 °C with two maxima at 490 and 680 °C, which correspond to the loss of C<sub>13</sub>H<sub>12</sub>N<sub>3</sub>O<sub>0.5</sub> fragment with an estimated mass loss of 25.02% (calculated mass loss = 25.15%). Finally, a residue of ½ Yb<sub>2</sub>O<sub>3</sub> oxide was expected to remain after the loss of all the organic fragments, which would result in an overall weight loss of 78.00% (calculated mass loss = 77.50%).

### 3.2 Structural interpretation

The structures of the synthesized metal complexes of the Schiff base ligand (HL) with La(III), Er(III) and Yb(III) were characterized by elemental analyses, molar conductance, magnetic and thermal analysis data. From IR spectra, it could be concluded that HL ligand behaved as a neutral tridentate ligand coordinated to the metal ions via three nitrogen atoms. From the molar conductance data, it was found that all the complexes have an electrolyte nature, and the structure of the formed complexes was shown in Figure-1.

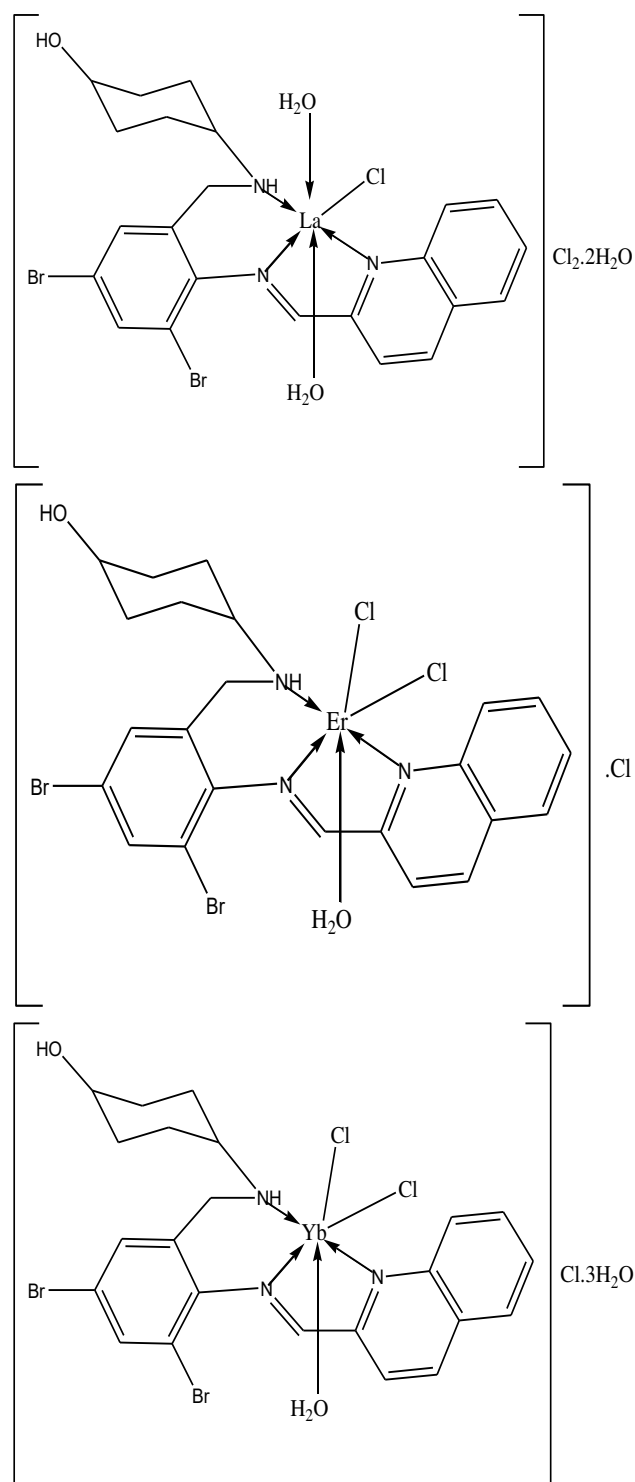


**Figure-1.** General Structure of the formed metal complexes.

### 3.3 Biological activity

For the Schiff base ligand (HL) and its metal complexes conducted in this paper, antibacterial and antifungal activities in vitro were screened against two bacteria species Gram-negative (*Salmonella* species and *Escherichia coli*), Gram-positive bacteria (*Bacillus subtilis* and *Staphylococcus aureus*) and two fungi species (*Aspergillus fumigatus* and *Candida albicans*). Figures (2,



3) showed the zone of inhibition measurements versus the growth of bacteria and fungi of the HL ligand and its metal complexes also their data was listed in Table-4. DMSO was used as a negative control and amikacin and

ketokonazole were used as positive standards for antibacterial and antifungal studies(Joseyphus and Nair, 2008; Kumaravel *et al.*, 2018).

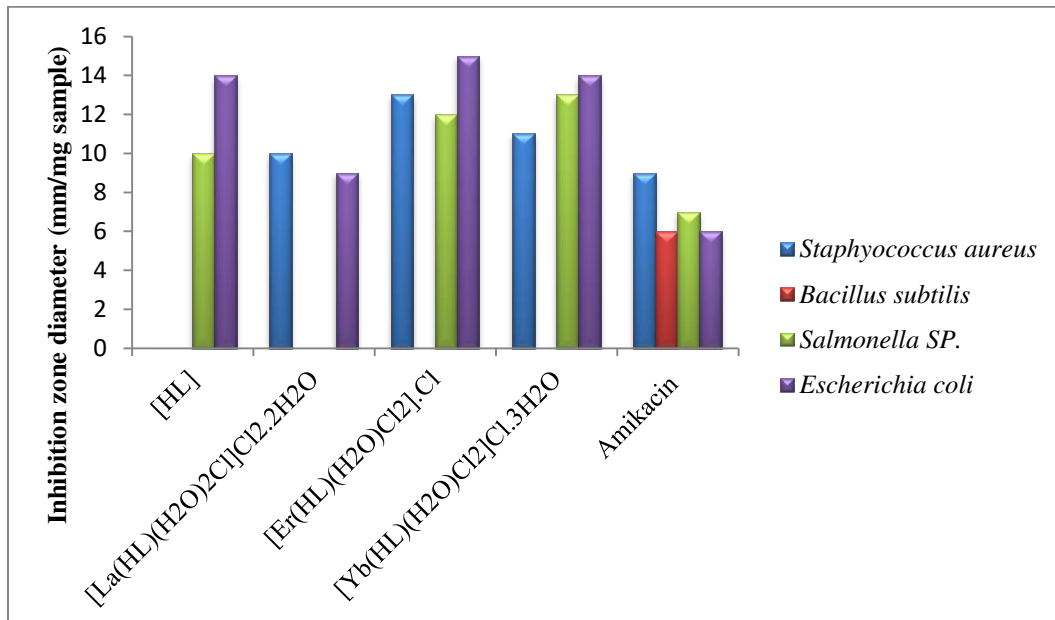


**Figure-2.** Biological activity of Schiff base ligand (HL) and its metal complexes with bacteria.

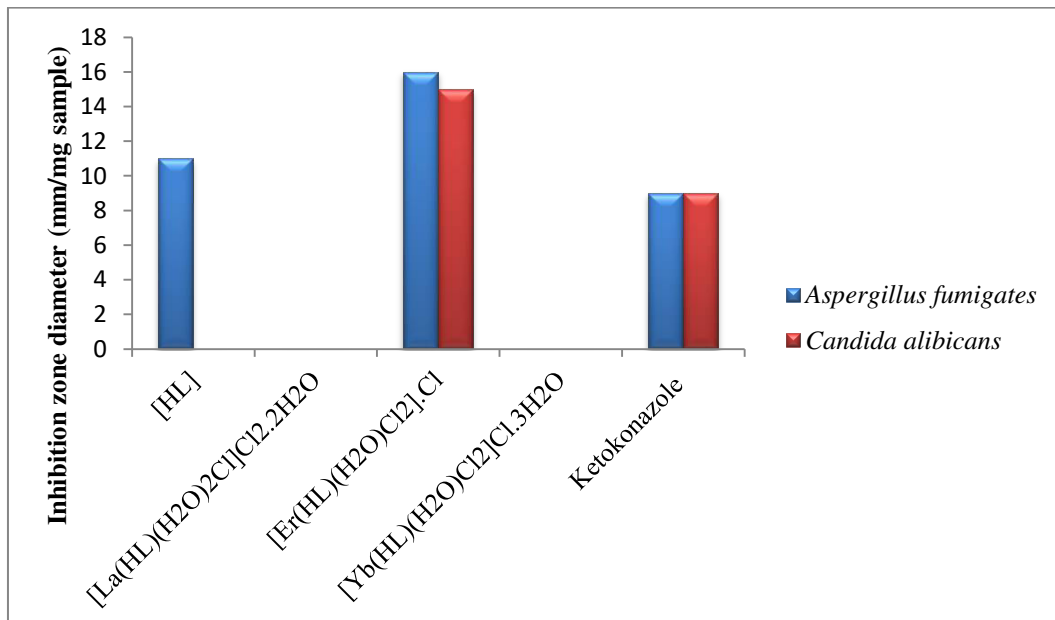


**Figure-3.** Biological activity of Schiff base ligand (HL) and its metal complexes with Fungi.

**Table-4.** Biological activity of HL ligand and its metal complexes.

Sample	Inhibition zone diameter (mm / mg sample)					
	Gram positive bacteria		Gram negative bacteria		Fungi	
	<i>Staphylococcus aureus</i>	<i>Bacillus subtilis</i>	<i>Salmonella species</i>	<i>Escherichia coli</i>	<i>Aspergillus fumigatus</i>	<i>Candida albicans</i>
[HL]	12	NA	13	12	12	11
[La(HL)(H <sub>2</sub> O) <sub>2</sub> Cl]Cl <sub>2</sub> .2H <sub>2</sub> O	10	NA	NA	9	NA	NA
[Er(HL)(H <sub>2</sub> O)Cl <sub>2</sub> ].Cl	13	NA	12	15	16	15
[Yb(HL)(H <sub>2</sub> O)Cl <sub>2</sub> ]Cl.3H <sub>2</sub> O	11	NA	13	14	NA	NA
Standard	Amikacin	9	6	7	6	---
	Ketokonazole	---	---	---	---	9
						9

Metal complexes recorded very high biological activity which may be attributed to the great lipophilic nature of them that can be explained on the basis of Overtone's concept and Tweedy's chelation theory (Fetoh *et al.*, 2019). According to the cell permeability concept of Overtone, the lipid membrane that surrounds the cell favored the passage of the lipid soluble materials only so liposolubility was considered to be a vital feature that controls the antimicrobial activity. The chelation process stated that, the great reduction in the metal ion polarity was related to the ligand orbital overlap and partial sharing of positive charge of metal ion with donor groups. Moreover, it increased the delocalization of the  $\pi$  electrons over the whole chelate ring and improved the lipophilicity of the complex. Upon this increase in lipophilicity, the penetration of the complexes into the lipid membrane will be enhanced as well as the metal binding sites on enzymes of microorganisms will be blocked. These metal complexes also had the ability to disturb the respiration process of the cell which will hinder the protein synthesis process resulting in the reduction of the organism growth. There are other factors which also may increase the activity including conductivity, solubility and bond length between the metal and ligand (Fetoh *et al.*, 2019; Kumaravel *et al.*, 2018).

The antibacterial studies showed that, by using *Staphylococcus aureus* as Gram-positive bacteria, the Er(III) complex had biological activity higher than that of the free ligand while La(III) and Yb(II) complexes had biological activity lower than that of the free ligand.

Using *Bacillus subtilis* as Gram-positive bacteria, both of the free ligand and all of its metal complexes didn't show any biological activity towards it.

Using *Salmonella species* as Gram-negative bacteria, both the ligand and its Yb(III) complex had the same biological activity which was higher than that of the Er(III) complex. On the other hand, La(III) complex didn't show any biological activity towards it.

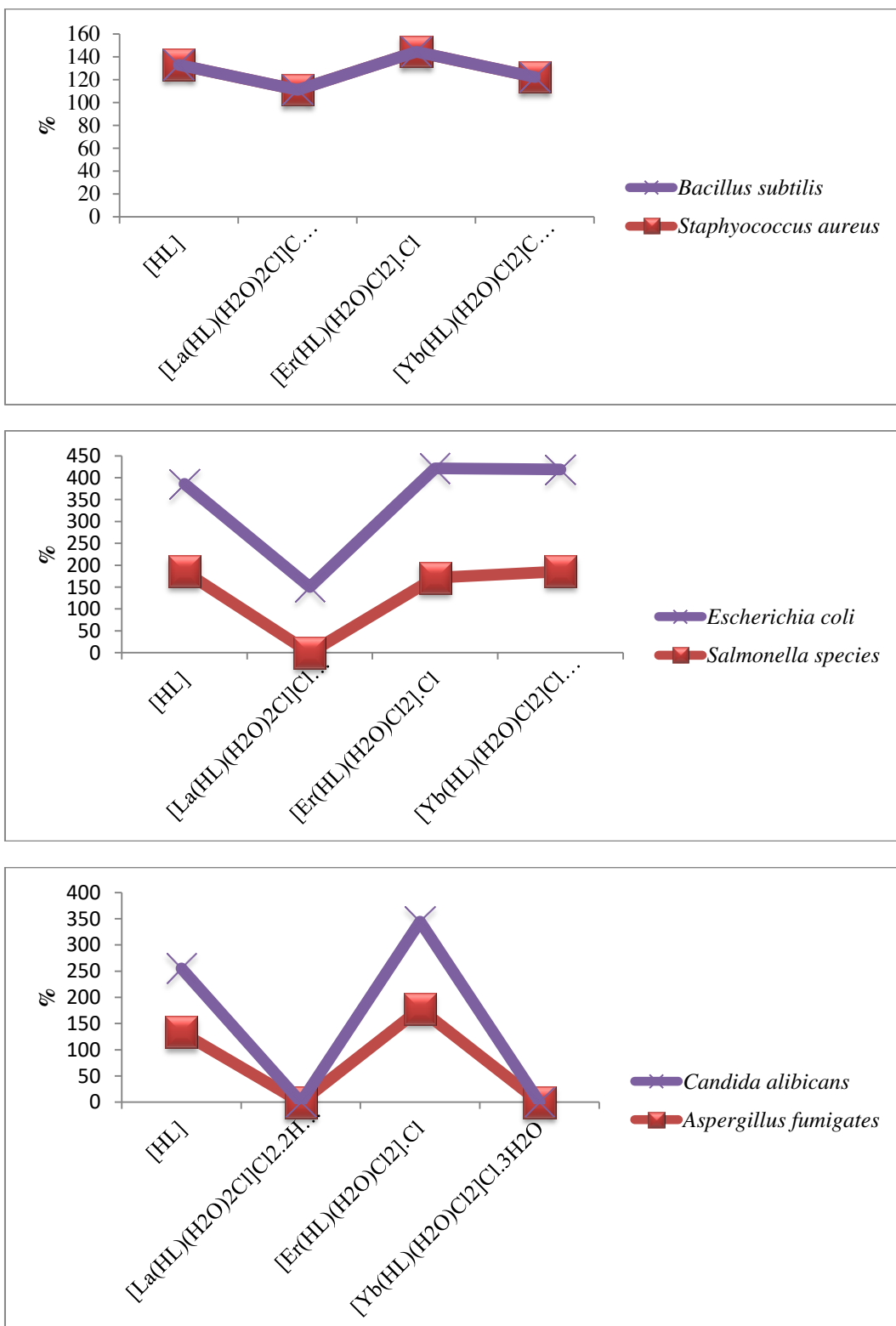
Using *Escherichia coli* as Gram-negative bacteria, both Er(III) and Yb(III) complexes had biological activity higher than the free ligand. While, the La(III) complex had biological activity lower than that of the free ligand.

The antifungal studies showed, by using *Candida albicans* and *Aspergillus fumigatus*, the Er(III) complex had biological activity higher than that of the free ligand. While both of La(III) and Yb(III) complexes didn't show any biological activity towards them.

The activities of the prepared Schiff base ligand and its metal complexes were confirmed by calculating the activity index according to the following relation(Balouiri *et al.*, 2016):

$$\text{Activity index (A)} = \left[ \frac{\text{Inhibition Zone of compound (mm)}}{\text{Inhibition Zone of standard drug (mm)}} \right] \times 100$$

From the previous data, it was concluded that almost Er(III) complex had the highest activity index for all the applied bacteria and fungi (Figure-4).

**Figure-4.** Activity index of HL ligand and its metal complexes.

#### 4. CONCLUSIONS

New La(III), Er(III) and Yb(III) complexes with the Schiff base ligand (HL) were prepared and characterized. The ligand acted as neutral tridentate through three nitrogen atoms and all the complexes showed octahedral geometry. All the complexes had an

electrolytic nature. From the data of elemental analysis, the complexes had composition of the MHL type with general formulae  $[M(HL)(H_2O)_2Cl]Cl_n.(H_2O)_m$  which was differentiated according to the metal ion. Almost Er(III) complex showed the highest biological activity index.



## REFERENCES

- Abdel-Monem Y., Abouel-Enein S. and El-Seady S. 2018. Synthesis, characterization and molecular modeling of some transition metal complexes of Schiff base derived from 5-aminouracil and 2-benzoyl pyridine. *J of Mol. Struc.* 1152, 115-27.
- Ahmadi R. and Amani S. 2012. Synthesis, Spectroscopy, Thermal Analysis, Magnetic Properties and Biological Activity Studies of Cu(II) and Co(II) Complexes with Schiff Base Dye Ligands. *Molec.* 17, 6434-48.
- Alshaheri A., Tahir M., Abdul Rahman M., Begum T. and Saleh T. 2017. Synthesis, characterisation and catalytic activity of dithiocarbazate Schiff base complexes in oxidation of cyclohexane. *J of Mol. Liq.* 240, 486-96.
- Arulmurugan S., Kavitha H. and Venkatraman B. 2010. Biological activities of schiff base and its complexes: a review. *Rasayan J. Chem.* 3, 385-410.
- Balouiri M., Sadiki M. and Ibnsouda S. 2016. Methods for in vitro evaluating antimicrobial activity: A review. *J Pharmaceutical Analysis.* 6, 71-9.
- Cakir U., Temel H., Ilhan S. and Ugras H. 2003. Spectroscopic and Conductance Studies of New Transition Metal Complexes with a Schiff Base Derived from 4-Methoxybenzaldehyde and 1, 2-bis (p Aminophenoxy) ethane. *Marcel Dekker, Inc.* 36, 429-40.
- Deghadi R., Mohamed G. and Mahmoud W. 2016. Novel Schiff base ligand and its metal complexes with some transition elements. Synthesis, spectroscopic, thermal analysis, antimicrobial and in vitro anticancer activity. *Appl. Organomet. Chem.* 30, 221-30.
- Dia M., El-Sonbati A., Shoair A., Eldesoky A. and El-Far N. 2017. Synthesis, structural, spectroscopic and biological studies of Schiff base complexes. *J of Mol. Struc.* 1141, 710-39.
- El-Binary A., El-Sonbati A., Diab M., El-Ghamaz N., Shoair A. and Nozha S. 2016. Potentiometric studies and molecular docking of Quinoline Schiff base and its metal complexes. *J Mater. Envir. Sci.* 6, 1934-47.
- Fetoh A., Asla K. A., El-Sherif A. A., El-Didamony H. and El-Reash G. M. A. 2019. Synthesis, structural characterization, thermogravimetric, molecular modelling and biological studies of Co(II) and Ni(II) Schiff bases complexes. *J of Mol. Struc.* 1178, 524-37.
- Gueye M., Dieng M., Thiam I., Lo, D., Barry, A., Gaye, M., and Retailleau, P. 2017. Lanthanide (III) Complexes with Tridentate Schiff Base Ligand, Antioxidant Activity and X-Ray Crystal Structures of the Nd(III) and Sm(III) Complexes. *S. Afr. J Chem.* 70, 8-15.
- Issa R., Khedr A. and Rizk H. 2008. 1H NMR, IR and UV/VIS Spectroscopic Studies of Some Schiff Bases Derived From 2-Aminobenzothiazole and 2-Amino-3-hydroxypyridine. *J of Chin. Chem. Soc.* 55, 875-84.
- Jenisha David S. and Priyadharsini J. 2015. Schiff base ligand its complexes and their ft-ir spectroscopy studies. *Int. J. on App. Bioeng.* 9, 1-4.
- Joseyphus R. and Nair M. 2008. Antibacterial and Antifungal Studies on Some Schiff Base Complexes of Zinc(II). *Mycobio.* 36, 93-8.
- Kumaravel G., Utthra P. and Raman N. 2018. Exploiting the biological efficacy of benzimidazole based Schiff base complexes with l-Histidine as a co-ligand: Combined molecular docking, DNA interaction, antimicrobial and cytotoxic studies. *Bioorganic Chem.* 77, 269-79.
- Mahmoud W., Khalil M., Elsayy H., Mohamed G. and Radwan M. 2017. Preparation, Characterization and Biological Activity Evaluation of some Metal Complexes from Novel Schiff Bases based on Ambroxol Drug. *Int. J of Advan. Sci. Res. and Man.* 2, 98-112.
- More G., Raut D., Aruna K. and Bootwala S. 2017. Synthesis, spectroscopic characterization and antimicrobial activity evaluation of new tridentate Schiff bases and their Co(II) complexes. *J of Saudi Chem. Soc.* 21, 954-64.
- Nassar M., Ahmed I., Dessouki H. and Ali S. 2018. Synthesis and characterization of some Schiff base complexes derived from 2, 5 Dihydroxyacetophenone with transition metal ions and their biological activity. *J of Basic and Envir. Sci.* 5, 60-71.
- Rajesh P., Gunasekaran S. and Manikandan A. 2017. Structural, spectral analysis of ambroxol using DFT methods. *J of Mol. Struc.* 1144, 379-88.
- Slassi S., Aarjane M., Yamni K. and Amine A. 2019. Synthesis, crystal structure, DFT calculations, Hirshfeld surfaces, and antibacterial activities of schiff base based on imidazole. *J of Mol. Struc.* 1197, 547-54.
- Zoubi W. A. and Ko, Y. 2017. Schiff base complexes and their versatile applications as catalysts in oxidation of organic compounds: part I. *Appl. Organometal. Chem.* 31, DOI 10.1002/aoc.3574.